

Variational Delay Metrics for Interconnect Timing Analysis

Kanak Agarwal, Dennis Sylvester, David Blaauw
University of Michigan, Ann Arbor

Frank Liu, Sani Nassif, Sarma Vrudhula*
IBM Research, Austin, *University of Arizona, Tucson

ABSTRACT

In this paper we develop an approach to model interconnect delay under process variability for timing analysis and physical design optimization. The technique allows for closed-form computation of interconnect delay probability density functions (PDFs) given variations in relevant process parameters such as linewidth, metal thickness, and dielectric thickness. We express the resistance and capacitance of a line as a linear function of random variables and then use these to compute circuit moments. Finally, these variability-aware moments are used in known closed-form delay metrics to compute interconnect delay PDFs. We compare the approach to SPICE based Monte Carlo simulations and report an error in mean and standard deviation of delay of 1% and 4% on average, respectively.

Categories and Subject Descriptors

B.7.2 [Integrated Circuits]: Design Aids, B.8.2 [Performance and Reliability]: Performance Analysis and Design Aids

General Terms

Performance, Design

1. INTRODUCTION

With process technologies shrinking to the nanometer regime, the impact of process variation on performance has become extremely critical [1]. Process variation can have a significant impact on both device (front-end of the line) and interconnect (back-end of the line) performance [2]. The effects of device parameter variations are typically captured by using a corner-based analysis. However, it has been shown that the corner-based analysis cannot be applied to interconnect due to their context dependent nature [3]. It was shown in [3] that for two different interconnect structures, when metal thickness is increased, the delay of the one structure increases while that of the other structure may reduce. This makes it very difficult to capture the impact of variability on interconnect delay using a traditional corner-based method.

Recently, work was proposed to capture the effect of interconnect variability on timing. Reference [4] proposes a reduced order modeling approach that includes manufacturing variations. The authors suggest an analytical framework to perform variational analysis using model order reduction approaches such as PRIMA [5]. However, the proposed approach is computationally

This work is supported by grants from NSF, GSRC, IBM and equipment donations from Intel and Sun.

Permission to make digital or hard copies of all or part of this work for personal or classroom use is granted without fee provided that copies are not made or distributed for profit or commercial advantage and that copies bear this notice and the full citation on the first page. To copy otherwise, or republish, to post on servers or to redistribute to lists, requires prior specific permission and/or a fee.

DAC'04, June 7–11, 2004, San Diego, California, USA

Copyright 2004 ACM 1-58113-828-8/04/0006...\$5.00.

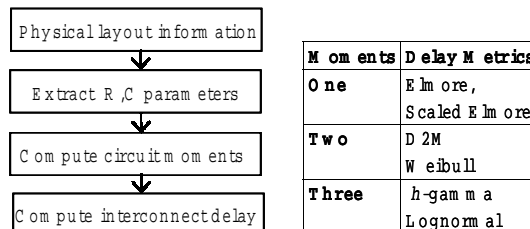


Figure 1: Basics of moment-based delay metrics

expensive due to the lack of closed-form expressions. A second drawback of the approach is that it can only be used to predict the change in interconnect delay due to deterministic values of the changes in the physical dimensions. In reality, the changes in the physical dimensions are not deterministic values but are random variables. Therefore, it is required that an interconnect analysis framework be developed that takes in probability density functions (PDFs) of the changes in physical dimensions and outputs the PDF of the change in the interconnect delay. In this paper, we propose a methodology to achieve this objective.

This type of statistical interconnect modeling approach should be computationally efficient in order to be useful in incremental timing analysis and physical design optimizations. This is the reason why there has been substantial effort in developing closed-form metrics for nominal interconnect delay calculation [7-11]. The existing delay modeling methodology and some of the existing moment-based metrics for delay computation are summarized in Figure 1. In this paper, we incorporate variability into these metrics and propose the use of closed-form *variational delay metrics* that can be used to efficiently predict the mean and variance of interconnect delay in the presence of uncertainty in the geometric dimensions.

2. VARIATIONAL INTERCONNECT METRICS

In this section we discuss our approach for modeling interconnect delay while considering variability in the physical dimensions. In our methodology, we express delay directly as a function of changes in the physical parameters. The advantages of such a formulation are that it preserves all correlations and that it can be very useful in evaluating delay sensitivities due to changes in various physical dimensions. Our approach is based on the observation that the interconnect delay distribution with process variation considered is Gaussian. This implies that interconnect delay can be expressed as a linear function of variations in physical dimensions. This point allows us to simplify complex expressions by truncating them to their linear terms. The basic methodology of delay computation remains the same as the conventional approach of Figure 1. The steps in our approach are summarized below. Each of these steps is then discussed in detail in the following sections.

1. Express electrical parameters (resistances and capacitances) in terms of *changes* in physical dimensions.

- Express moments in terms of electrical parameters and hence in terms of changes in physical dimensions.
- Express interconnect delay as a function of moments and therefore in terms of changes in physical dimensions. Find mean and variance of delay distribution as a function of the statistics of variability in physical dimensions.

For simplicity, in the following discussion, we consider variations only in metal width (W), metal thickness (T) and interlayer dielectric thickness (H). We explain our approach for these three dimensions but there is no restriction on the number of variables in our methodology. The approach can be easily extended to include other variation sources. We assume that the geometric variations are expressed as Gaussian distributions and that variation in one dimension is mutually independent with variations in other dimensions.

2.1 Mapping Physical Dimensions to Electrical Parameters

To first order, delay through an interconnect can be expressed as the RC product of its resistance and capacitance. With any change in the physical dimensions of the wire, its resistance and capacitance also change, causing interconnect delay to fluctuate. In order to model the impact of variability on wire delay, we need to capture the effect of geometric variations on the electrical parameters. The change in electrical parameters due to variations in geometric dimensions can be captured by the simple linear approximation shown in Equation 1:

$$\begin{aligned} R &= R_{nom} + a_1 \Delta W + a_2 \Delta T \\ C &= C_{nom} + b_1 \Delta W + b_2 \Delta T + b_3 \Delta H \end{aligned} \quad (1)$$

Here, R_{nom} and C_{nom} represent nominal resistance and capacitance values, computed when the wire dimensions are at their nominal or typical values. ΔW , ΔT , and ΔH represent the change in metal width, metal thickness, and ILD thickness respectively. The coefficients a_i and b_i are the modeling coefficients in the linearized model. This linear approximation shows a high degree of accuracy for our purpose while remaining very simple to use. Linear models similar to Equation 1 have been proposed in earlier works on interconnect variability [12]. Reference [12] proposes a methodology that requires a one-time nominal capacitance extraction after which look-up tables are used to calculate delta capacitances due to geometric parameter variations. In this paper, we use empirical capacitance modeling equations [13] to compute linear coefficients but any look-up table-based linear modeling approach can be used in a similar manner. We now discuss how these electrical parameters can be mapped to the moments.

2.2 Mapping Electrical Parameters to Moments

Once interconnect dimensions are mapped to the circuit parameters, the next step is the computation of circuit moments. For deterministic resistance and capacitance values in an RC tree, the circuit moments can be computed easily by path tracing [6]. However, with interconnect variability the resistances and capacitances are now random variables. If changes in physical dimensions (ΔW , ΔT , etc.) are considered independent normal random variables, then the resistance and capacitance calculated using Equation 2 are correlated normal random variables. This adds complexity in the moment computation process especially for higher order moments. We illustrate moment computation with variability for the simple RC tree example shown in Figure 2.

The first moment at any node can be expressed as a function of resistances R_i 's and capacitances C_i 's. For example, the first moment at node 3 (without considering variability) in the above circuit is given by

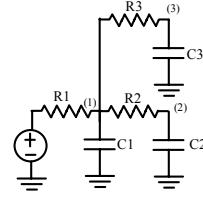


Figure 2: A simple RC tree

$$m_1^3 = m_1(R_i, C_i) = -R_1(C_1 + C_2 + C_3) - R_3C_3 \quad (2)$$

With variability, the resistances R_i and the capacitances C_i are linear functions of random variables (ΔW , ΔT , etc).

$$\begin{aligned} R_i &= R_{i(nom)} + R_{i(W)}\Delta W + R_{i(T)}\Delta T \\ C_i &= C_{i(nom)} + C_{i(W)}\Delta W + C_{i(T)}\Delta T + C_{i(H)}\Delta H \end{aligned} \quad (3)$$

Here, $R_{i(nom)}$ and $C_{i(nom)}$ are nominal resistance and capacitance respectively. The coefficients $R_{i(W)}$, $C_{i(W)}$ model change in the resistance and capacitance with a change in width. Similarly, other coefficients capture the delta resistance and delta capacitance with respect to each physical dimension. All such coefficients can be computed as discussed in Section 2.1. Substituting R_i and C_i from Equation 3 into Equation 2 gives

$$\begin{aligned} m_1 &= m_{1(nom)} + k_W\Delta W + k_T\Delta T + k_H\Delta H + k_W^2(\Delta W)^2 \\ &\quad + k_T^2(\Delta T)^2 + k_{WT}(\Delta W\Delta T) + k_{WH}(\Delta W\Delta H) + k_{TH}(\Delta T\Delta H) \end{aligned} \quad (4)$$

Here $m_{1(nom)}$ is the first moment evaluated at nominal resistance $R_{i(nom)}$ and nominal capacitance $C_{i(nom)}$. We express this by the following notation:

$$m_{1(nom)} = m_1(R_{i(nom)}, C_{i(nom)}) \quad (5)$$

The coefficients in Equation 4 can be calculated by evaluating the first moment at different values of R 's and C 's. For example, the coefficient k_W^2 can be computed by calculating the first moment when all resistances and capacitances are replaced by the corresponding $R_{i(W)}$ and $C_{i(W)}$. The expressions for each coefficient in terms of first moment computation are given below.

$$\begin{aligned} k_W &= m_1(R_{i(W)}, C_{i(nom)}) + m_1(R_{i(nom)}, C_{i(W)}) & k_{W^2} &= m_1(R_{i(W)}, C_{i(W)}) \\ k_T &= m_1(R_{i(T)}, C_{i(nom)}) + m_1(R_{i(nom)}, C_{i(T)}) & k_{T^2} &= m_1(R_{i(T)}, C_{i(T)}) \\ k_H &= m_1(R_{i(nom)}, C_{i(H)}) & k_{WH} &= m_1(R_{i(W)}, C_{i(H)}) \\ k_{WT} &= m_1(R_{i(W)}, C_{i(T)}) + m_1(R_{i(T)}, C_{i(W)}) & k_{TH} &= m_1(R_{i(T)}, C_{i(H)}) \end{aligned} \quad (6)$$

Equation 4 shows the first moment expression as a function of normal random variables representing variations in back-end physical dimensions. Equation 4 contains higher order terms and cross product terms, thereby implying that the distribution of first moments is not exactly Gaussian. However, experimentally, we find that the higher order terms are not significant and can be neglected without loss of accuracy (results are detailed later in this section). By neglecting higher order terms, the first moment expression from Equation 4 reduces to the following equation:

$$m_1 = m_{1(nom)} + k_W\Delta W + k_T\Delta T + k_H\Delta H \quad (7)$$

We can perform a similar analysis for the second moment. The second moment can be expressed as a function of resistances, capacitances, and the first moments. For example, the second moment at node 3 (without considering variability) for the circuit in Figure 2 is given by

$$m_2^3 = m_2(R_i, C_i, m_1^i) = -R_1(m_1^1C_1 + m_1^2C_2 + m_1^3C_3) - R_3(m_1^3C_3) \quad (8)$$

With variations in physical dimensions, R_i 's and C_i 's can be replaced by their corresponding expressions from Equation 3 and similarly m_1 's can be replaced by the expression given in Equation 7. If we again keep only the linear terms, m_2 can be expressed as

$$m_2 = m_{2(nom)} + A_W \Delta W + A_T \Delta T + A_H \Delta H \quad (9)$$

Here $m_{2(nom)}$ is the second moment evaluated at nominal resistance $R_{i(nom)}$, nominal capacitance $C_{i(nom)}$ and nominal first moment $m_{1(nom)}$. We express this by following notation.

$$m_{2(nom)} = m_2(R_{i(nom)}, C_{i(nom)}, m_{1(nom)}) \quad (10)$$

The coefficients in Equation 9 can be calculated by evaluating the second moment at different values of R 's, C 's and m_1 's.

$$\begin{aligned} A_W &= m_2(R_{i(nom)}, C_{i(nom)}, k_W) + m_2(R_{i(nom)}, C_{i(W)}, m_{1(nom)}) \\ &\quad + m_2(R_{i(W)}, C_{i(nom)}, m_{1(nom)}) \\ A_T &= m_2(R_{i(nom)}, C_{i(nom)}, k_T) + m_2(R_{i(nom)}, C_{i(T)}, m_{1(nom)}) \\ &\quad + m_2(R_{i(T)}, C_{i(nom)}, m_{1(nom)}) \\ A_H &= m_2(R_{i(nom)}, C_{i(nom)}, k_H) + m_2(R_{i(nom)}, C_{i(H)}, m_{1(nom)}) \end{aligned} \quad (11)$$

Here k_W , k_T , and k_H can be computed as shown in Equation 6. We again point out that Equations 9 and 11 show only the linear coefficients. We can write a full expression of the second moment (similar to Equation 4 for the first moment), however we again find that the non-linear terms are not significant and can be ignored.

To test the linearity assumption, we reconsider a simple 5 mm long line with a ground plane below the line. Nominal metal width and thickness of the line were chosen to be $0.8\mu\text{m}$ and nominal ILD thickness was $0.55\mu\text{m}$. We considered a 3-sigma tolerance of $\pm 0.1\mu\text{m}$ in width and thickness and $\pm 0.05\mu\text{m}$ in ILD thickness. Given these distributions of ΔW , ΔT , and ΔH , we plot the distributions of first and second moments at sink node with and without the non-linear terms. Figure 3 shows that the two curves are almost identical. The figures also show that the distributions of moments are Gaussian and hence the linear approximations of Equation 7 and 9 are extremely accurate.

To this point we have provided expressions for the first and second circuit moments as a function of random variables (ΔW , ΔT , etc.). We have also shown that the moments have Gaussian distributions and the complicated expressions of the moments can be safely truncated to contain only linear terms. This allows us to keep the expressions simple and tractable. Furthermore we have demonstrated that the coefficients in the expressions of the moments can be easily computed in a manner similar to the nominal moment computation. We now turn our attention to mapping circuit moments to the delay metrics.

2.3 Mapping Moments to Delay Metrics

Once moments are expressed as functions of change in physical dimensions, the next step is to map the PDF of these moments to an interconnect delay PDF. Among existing delay metrics, we chose D2M [8] for our analysis in this paper. We explain our methodology for D2M but the approach is independent of the metric and can be applied to any other closed-form metric as well.

Using D2M the delay in terms of moments can be expressed as

$$D2M = \ln 2 * \frac{(m_{1(nom)} + k_W \Delta W + k_T \Delta T + k_H \Delta H)^2}{\sqrt{m_{2(nom)} + A_W \Delta W + A_T \Delta T + A_H \Delta H}} \quad (12)$$

Analyzing the D2M expression in Equation 12 is difficult. However, if we write a series expansion of the expression and keep only the linear terms, then the D2M expression can be re-written as

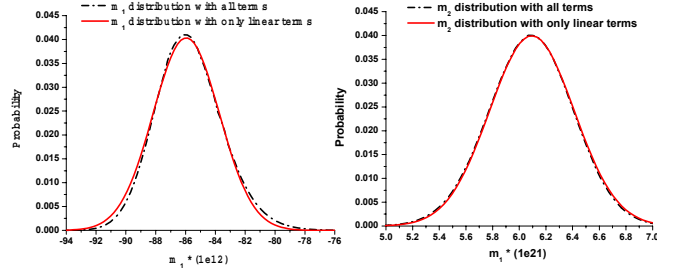


Figure 3: First (left plot) and second (right plot) moment distributions with and without considering non-linear terms.

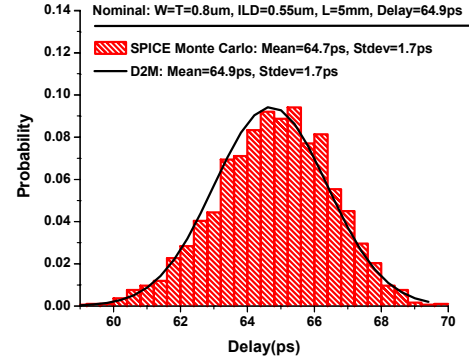


Figure 4: Delay distribution using statistical D2M compared to Monte Carlo simulations.

$$D2M = \ln 2 * \frac{(m_{1(nom)})^2}{\sqrt{m_{2(nom)}}} (1 + S_W \Delta W + S_T \Delta T + S_H \Delta H) \quad (13)$$

Here S_W , S_T , and S_H can be calculated using

$$S_W = \frac{2k_W}{m_{1(nom)}} - \frac{A_W}{2m_{2(nom)}} \quad S_T = \frac{2k_T}{m_{1(nom)}} - \frac{A_T}{2m_{2(nom)}} \quad S_H = \frac{2k_H}{m_{1(nom)}} - \frac{A_H}{2m_{2(nom)}} \quad (14)$$

To test the above expression, we reconsider the test case used in Figure 3. We performed 1000 Monte Carlo simulations and measured 50% delay in each case. Figure 4 shows the distribution of delay measured from the simulations. The figure also shows the PDF for delay generated using Equation 13. It is clear from the figure that Gaussian nature of the delay distribution is captured well by the statistical D2M model.

Equation 13 is a simple linear function of ΔW , ΔT , and ΔH . If ΔW , ΔT and ΔH are independent random variables with their mean values zero and standard deviations of σ_W , σ_T , and σ_H respectively, then the mean and standard deviation of delay in terms of the standard deviations in physical dimensions can be written as

$$\begin{aligned} E(D2M) &= \ln 2 * \frac{(m_{1(nom)})^2}{\sqrt{m_{2(nom)}}} \\ Stdev(D2M) &= \ln 2 * \frac{(m_{1(nom)})^2}{\sqrt{m_{2(nom)}}} \sqrt{(S_W^2 \sigma_W^2 + S_T^2 \sigma_T^2 + S_H^2 \sigma_H^2)} \end{aligned} \quad (15)$$

For the example of Figure 4, the mean and standard deviation of delay computed using Equation 15 are 64.9ps and 1.7ps respectively. These numbers match well with the 64.7ps and 1.7ps found using Monte-Carlo simulations. The advantage of Equation 13 lies in its simplicity, making it useful in evaluating delay sensitivity to variation in a particular physical dimension.

3. EXPERIMENTAL RESULTS

In this section, we test our methodology on various test cases. First, we test the Gaussian assumption (and hence the linearity assumption) when the variations in physical dimensions are large. We chose a simple line with nominal metal width and thickness of $0.6\mu\text{m}$ and nominal ILD thickness of $0.45\mu\text{m}$. We considered 3-sigma variations of 30% in all the three dimensions, which is slightly larger than the expected levels of back-end process variability [1]. Figure 5 compares the delay distribution using our approach with Monte Carlo simulations. The figure shows that even with large variations in geometric dimensions the delay distribution remains Gaussian, and the proposed model captures its mean and variance very accurately.

For the next experiment, we revisit the test case discussed in Figures 3-4. Modeling this 5mm line using 30 identical segments, we look at the various nodes along the line and compute their distributions. Table I compares the mean and standard deviation computed using Monte Carlo simulations with the proposed model. The table shows that the model works well across all nodes. Node 10 shows a relatively large error in the mean and variance computation, but this error is primarily due to the error in D2M in nominal delay calculation for near-end nodes. Table I also shows the nominal delay computed using SPICE. We observe here that the means computed using Monte Carlo simulations are very close to the nominal delays for all the nodes, thereby implying that the Gaussian assumption is applicable for intermediate nodes as well.

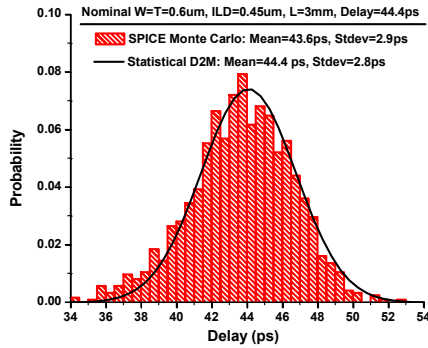


Figure 5: Delay distribution using statistical D2M compared to Monte Carlo simulations

Table I: Mean and standard deviation of delay distribution along various nodes in a simple 30-segment line

Node	Nom Delay (ps) (SPICE)	Mean (ps)		Stdev (ps)	
		SPICE	Model	SPICE	Model
10	20.9	20.8	28.2	0.56	0.73
15	41.1	40.9	43.4	1.1	1.12
20	55	54.8	55.2	1.46	1.43
25	62.5	62.3	62.6	1.67	1.63
30	64.9	64.7	64.9	1.71	1.69

Table II: Error statistics on 2900 test cases

2900 testcases	Mean (Delay)	Stdev (Delay)
Avg. Error	1.2%	3.8%
Error Bins	Mean(Delay)	Stdev(Delay)
<1%	31.7%	15.7%
<2%	92.3%	33.9%
<5%	100%	75.5%

We also generated a large set of random test cases by varying nominal physical dimensions and their 3-sigma variabilities. Nominal linewidths and thicknesses were allowed to vary from $0.4\mu\text{m}$ to $0.8\mu\text{m}$ while nominal ILD thickness could take values between $0.25\mu\text{m}$ and $0.55\mu\text{m}$. For each test case, the 3-sigma variability in each of the three physical dimensions was randomly chosen to be between 10% and 30% of the nominal. Table II shows the error statistics for these 2900 test cases compared to Monte Carlo simulations. The 3-sigma variation in delay for this set of test cases ranged from 5% to 34% of the mean. This implies that even with the reverse trends shown by resistance and capacitance for a given change in physical dimensions, the delay variability due to back-end process tolerances can be large and should be modeled accurately.

4. CONCLUSIONS

We describe a simple technique to extend popular closed-form moment-based delay metrics to consider back-end process variation. These variational delay metrics are based on the use of linearized models of electrical parameters (R,C) that capture uncertainty in process parameters. These models are then used to compute moments using known path-tracing techniques – a key point is that only terms linear with the random variables (W,T,H) were found to be necessary to ensure good accuracy. These variation-aware moments were then used in accurate delay metrics such as D2M to capture the distribution of interconnect timing. We demonstrate good accuracy in the mean and standard deviation of the resulting interconnect delay distribution for a number of test cases (1.2% and 3.8% average error, respectively, for 2900 randomly generated test cases).

REFERENCES

- [1] S. R. Nassif, "Modeling and Analysis of Manufacturing Variations," *CICC*, pp. 223-228, 2001.
- [2] Z. Lin, C. Spanos, L. Milor, and Y. Lin, "Circuit Sensitivity to Interconnect Variation," *IEEE Trans. on Semiconductor Manufacturing*, v. 11, pp. 557-568, Nov. 1998.
- [3] Y. Liu, S. R. Nassif, L. T. Pileggi, and A. J. Strojwas, "Impact of Interconnect Variations on the Clock Skew of a Gigahertz Microprocessor," *DAC*, pp. 168-171, 2000.
- [4] Y. Liu, L. T. Pileggi, and A. J. Strojwas, "Model Order Reduction of RC(L) Interconnect Including Variational Analysis," *DAC*, pp. 201-206, 1999.
- [5] A. Odabasioglu, M. Celik, and L.T. Pileggi, "PRIMA: Passive reduced-order interconnect macromodeling algorithm," *ICCAD*, pp. 58-65, 1997.
- [6] C.L. Ratzlaff, N. Gopal, and L.T. Pillage, "RICE: Rapid Interconnect Circuit Evaluator," *DAC*, pp. 555-560, 1991.
- [7] W.C. Elmore, "The transient response of damped linear networks with particular regard to wideband amplifiers," *J. Applied Physics*, v. 19, pp. 55-63, Jan. 1948.
- [8] C. Alpert, A. Devgan, and C. Kashyap, "A two moment RC delay metric for performance optimization," *ISPD*, pp. 69-74, 2000.
- [9] K. Agarwal, D. Sylvester, and D. Blaauw, "Simple Metrics for Slew Rate of RC Circuits Based on Two Circuit Moments," *DAC*, pp. 950-953, 2003.
- [10] F. Liu, C. Kashyap, and C. Alpert, "A delay metric for RC circuits based on the Weibull distribution," *ICCAD*, pp. 620-624, 2002.
- [11] T. Lin, E. Acar, and L. Pileggi, "h-gamma: An RC delay metric based on a gamma distribution approximation to the homogenous response," *ICCAD*, pp. 19-25, 1998.
- [12] V. Mehrotra, S. Nassif, D. Boning, and J. Chung, "Modeling the Effects of Manufacturing Variation on High-Speed Microprocessor Interconnect Performance," *IEEE Electron Devices Meetings*, pp. 767-770, 1998.
- [13] J. Chern, J. Huang, L. Arledge, P. Li, and P. Yang, "Multilevel Metal Capacitance Models for CAD Design Synthesis Systems," *IEEE Electron Devices Letters*, pp. 32-34, Jan. 1992.